# Dielectrophoretic Forces and Potentials Induced on Pairs of Cells in an Electric Field

Kenneth R. Foster* and Arthur E. Sowers‡
*Department of Bioengineering, University of Pennsylvania, Philadelphia, Pennsylvania 19041-6021, and ‡Department of Pathology, School of Medicine, University of Maryland, Baltimore, Maryland 21201-1596 USA

ABSTRACT A combined numerical/experimental study is reported of the membrane potentials and dielectrophoretically induced forces between cells, membrane pressures, and velocity of attraction of cells under the influence of an electric field. This study was designed to explore electrical and mechanical effects produced by a field on cells in close proximity or undergoing electrically induced fusion. Laplace's equation for pairs of membrane-covered spheres in close proximity was solved numerically by the boundary element method, and the electrically induced forces on the cells and between cells were obtained by evaluating the Maxwell stress tensor. The velocity of approach of erythrocyte ghosts or fused ghosts in a 60-Hz field of 6 V/mm was measured experimentally, and the data were interpreted by using Batchelor's theory for hydrodynamic interaction of hard spheres. The numerical results show clearly the origin of the dielectrophoretic pressures and forces in fused and unfused cells and the effects of a nearby cell on the induced membrane potentials. The experimental results agree well with predictions based on the simple electrical model of the cell. The analysis shows the strong effect of hydrodynamic interactions between the cells in determining their velocity of approach.

## INTRODUCTION

It is well known that electric fields can induce forces on cells, which can lead to the deformation of cells, aggregation of cells, and cell fusion (Saito et al., 1966; Schwan, 1982; Sowers, 1993). These forces arise from the interaction of the external field and the induced dipole moment in the cell (Foster et al., 1992; Pastushenko et al., 1988; Sauer, 1983, 1985) and can be interpreted in terms of classical electromagnetic theory.

This present study has two chief motivations. First, Sowers and colleagues have recently studied the mechanical responses of red cells in electric fields, in particular the change in shape of pairs of cells after electrofusion (Wu et al., 1994), and the rate of approach of cells under the influence of the field (Dimitrov et al., 1990). The former experiments can be used to probe the mechanical properties of the cell membrane. Our first motivation is to gain an understanding of the electrically induced forces on the cells, which is needed for quantitative analysis of these experiments. The latter experiments can yield information about the electrical properties of cells in a very simple manner. However, as we discuss below, the experiments yielded anomalously high values for the effective conductivity of the cells. Our second motivation was to clarify this problem.

We model the cells as shell-surrounded spheres and numerically solve Laplace's equation to determine the electric fields and (by evaluating the Maxwell stress tensor) the field-induced forces on the system. This simple electrical model of the cell is appropriate if the Debye length of the electrolyte is small compared with other distance scales of interest. More elaborate models (e.g., Grosse and Schwan, 1992) might be needed to account for counterion effects and other phenomena that are likely to be important with low-frequency fields. Nevertheless, simple macroscopic models based on Laplace's equation have been remarkably successful for interpreting many bioelectric phenomena (Cole, 1972).

The present study has three related parts: numerical calculation of the induced fields and mechanical forces on pairs of fused or unfused cells in an electric field, numerical calculation of the forces between cells induced by the field, and consideration of the hydrodynamic problem of rate of approach of the cells. The second part of this study is a sensitive test of the accuracy of the calculations.

## THEORY

Fig. 1 shows two membrane-covered spheres, used to model biological cells. The spheres have outer and inner radii $r_{out}$ and $r_{in}$, respectively, and their centers are separated by a distance $h$. The inner and outer media and shell have conductivity ($\sigma_1$, $\sigma_2$) and permittivity ($\epsilon_1$, $\epsilon_2$), respectively. The spheres are located in an originally uniform electric field $E$.

### Calculation of fields

We calculated the electric fields in and near the spheres, using the program Electro from Integrated Engineering Software, Inc. (Winnipeg, Manitoba). This program employs the boundary element method, which is based on an integral formulation of Laplace's equation. It is limited to two-dimensional problems or to three-dimensional prob-

*Received for publication 18 July 1994 and in final form 21 February 1995.*
Address reprint requests to Dr. Kenneth R. Foster, Department of Bioengineering, University of Pennsylvania, 220 South 33rd Street, Philadelphia, PA 19104-6392. Tel.: 215-898-8534; Fax: 215-573-2071; E-mail: Kfoster@eniac.seas.upenn.edu. A.E.S. E-mail: arthures@access.digex.net.

0006-3495/95/09/777/08 $2.00

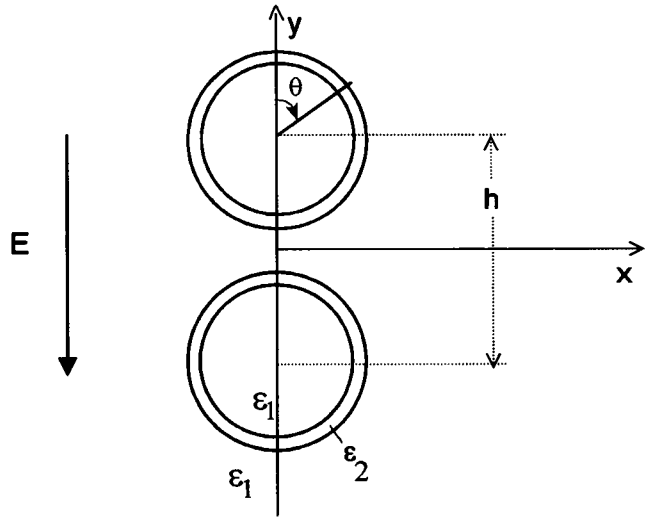


FIGURE 1. Geometry of two cells: outer and inner radii $r_{out}$ and $r_{in}$, separation of centers $h$. The thickness of the membrane is greatly exaggerated in this illustration.

lems when there is an axis of rotational symmetry (Foster, 1993).

For the present calculations the geometry of the problem was chosen to have an axis of rotational symmetry about the $y$ axis. Approximately 150 boundary elements were placed along each surface of the spheres. The external field was created by placing two parallel conductors at fixed potential, separated by the spheres by a distance of 7–15 particle diameters. We repeated the calculations at different values of the normalized separation $\gamma = h/r_{out}$, including the cases of touching particles ($\gamma = 2$) and of fused particles ($\gamma = 2$, with a small aperture, corresponding to 0.5% of the diameter of the sphere, connecting the particles).

The calculations used the time-independent mode of the program and are thus independent of the permittivity of the materials. This static calculation is appropriate for cells at frequencies below the beta relaxation frequency, which typically occurs near 1 MHz for cells in normal physiological media (Foster and Schwan, 1989). These numerical calculations can be extended readily for alternating frequencies, and we extend the formalism below for that case.

## Calculation of forces

The forces on the cell were obtained by numerical evaluation of the Maxwell stress tensor **T** (Panofsky and Phillips, 1962; Winterhalter and Helfrich, 1988). The elements of **T** in medium $I$ are

$$T_{l,m}^{(i)} = \epsilon_i \left[ E_l^{(i)} E_m^{(i)} - \frac{1}{2}(E^{(i)})^2 \delta_{l,m} \right], \tag{1}$$

where $E_l^{(i)}$ is the $i$th component of the electric field in medium $i$, $\epsilon_i$ is the permittivity of medium $i$, and $\delta_{l,m}$ is the Dirac delta function. This tensor must be evaluated on both sides of each interface, i.e., four times for a membrane-covered sphere.

Equation 1 can be simplified by using the boundary conditions on the normal and tangential components of the electric field ($E_r$ and $E_\theta$). At each interface, $(\sigma + j\omega\epsilon)E_r$ and $E_\theta$ are continuous, where $\sigma$ is the conductivity, $\omega$ is the radian frequency, and $\epsilon$ is the permittivity. Because the shell is assumed to be nonconductive, as $\omega \to 0$ the radial component of the electric field in the medium vanishes at the membrane surface. Under these assumptions, Eq. 1 yields force densities (force per unit area)

$$\mathrm{df}_r^{out} = \frac{1}{2}(E_\theta^2(\epsilon_2 - \epsilon_1) - \epsilon_2(E_r^{sh})^2),$$
$$\mathrm{df}_\theta^{out} = \epsilon_2 E_\theta E_r^{sh} \tag{2}$$

at the outer surface and

$$\mathrm{df}_r^{in} = \frac{1}{2}\epsilon_2(E_r^{sh})^2, \tag{3}$$
$$\mathrm{df}_0^{in} = 0$$

at the inner surface of the cell, where $E^{sh}$ is the field in the shell. For a thin shell, the net force per incremental surface area $ds$ is then

$$\mathrm{df}_r = \frac{1}{2}[\epsilon_2((E_r^{sh,\,in})^2 - (E_r^{sh,\,out})^2) + (E_\theta^{out})^2(\epsilon_2 - \epsilon_1)],$$
$$\mathrm{df}_\theta = -\epsilon_2 E_\theta^{out} E_r^{sh,\,out}. \tag{4}$$

The net force **F** on the cell can be obtained by integrating the Maxwell stress tensor over a single surface that encloses it (Stratton, 1941):

$$\mathbf{F} = \int_s \left[ \epsilon_1 \mathbf{E}^{out}(\mathbf{E}^{out} \cdot \mathbf{n}) - \frac{\epsilon}{2}(E^{out})^2 \mathbf{n} \right] ds, \tag{5}$$

where $s$ is the outer surface of the particle and the fields and permittivities are those in the outer medium. Equation 5 simplifies to

$$F_y = -\pi r_{out}^2 \epsilon_1 \int_0^\pi (E_\theta^{sh,\,out})^2 \cos(\theta)\sin(\theta)\,d\theta. \tag{6}$$

There will be no net force on an isolated cell from an initially uniform (alternating) external field. However, the presence of another cell nearby will perturb the field and lead to a net force of attraction between them. These forces arise from the interaction between the induced dipole moments in each cell and are to be distinguished from electrophoretic forces, which arise from the interaction between a field and a charged particle.

For an isolated membrane covered sphere in an originally uniform field $E$, solution of Laplace's equation yields (Foster and Schwan, 1989)

$$E_\theta^{out} = 1.5E\sin(\theta),$$
$$E_r^{sh,\,in} - E_r^{sh,\,out} = 3E\cos(\theta), \quad (7)$$
$$E_r^{sh,\,out} + E_r^{sh,\,in} = 3E\cos(\theta)R/d,$$

where $R = (r_{out} + r_{in})/2$ and $d = (r_{out} - r_{in})$ is the membrane thickness. This solution is correct to first order in $d/R$. To the same approximation, the net force densities on an incremental area ds of membrane are

$$df_r = \frac{9E^2}{2}\frac{R}{d}\epsilon_2\cos^2(\theta) = \frac{9E^2}{2}RC_m\cos^2(\theta),$$
$$df_\theta = \frac{-9}{4}E^2\frac{R}{d}\epsilon_2\cos(\theta)\sin(\theta) = \frac{-9}{4}E^2RC_m\cos(\theta)\sin(\theta), \quad (8)$$

where $C_m$ is the membrane capacitance. In the discussion below, the membrane forces are normalized by a factor $9E^2\epsilon_2R/2d$, the fields are normalized by the external field $E$, and the membrane potentials are normalized by $(3/2)E/R$.

## EXPERIMENTAL

The dielectrophoretic forces of attraction were measured between erythrocyte ghosts or pairs of erythrocyte ghosts. Experiments were conducted i) between two individual ghosts, ii) between a single ghost and two (nonfused) ghosts already in contact, and iii) between a single ghost and two fused ghost membranes.

The experiments were carried out on ghost membranes prepared and measured in 20-mM sodium phosphate buffer (pH 8.5, conductivity 260 mS/m). The methods were similar to that described previously (Dimitrov et al., 1990), with the addition of phase optics light microscopy to image the cells as described in Wu et al. (1994). In the experiments using fused pairs of erythrocyte ghosts, the cells were fused by a single dc field pulse (600 V/mm, 0.55-ms decay half-time), applied just before the attraction experiments were started. All experiments employed constant 60-Hz sinusoidal electric fields (6 V/mm rms) to induce dielectrophoretic forces. Measurements were made only on ghosts that were spherical in shape (erythrocyte ghosts as normally prepared have a continuous range of shapes from spherocytes to stomatocytes) and on pairs of cells whose centers formed a vector parallel to the electric field. The images of the cells were recorded on video tape and subsequently analyzed using the JAVA software package (Jandel Scientific, Corte Madera, CA).

## RESULTS

The forces were calculated on one of a pair of cells at various normalized separations $\gamma = h/R$. The numerical calculations assumed the following parameters:

$E$ = 1 (unperturbed external field strength, V/m),
$r_{out}$ = 1 (outer radius, m),
$r_{in}$ = 0.95 (inner radius, m),
$\sigma_1$ = 1 (conductivity of inner and outer media, S/m),
$\sigma_2$ = $10^{-5}$ (conductivity of shell, S/m),
$\epsilon_1$ = $80\epsilon_o$ (permittivity of inner and outer media), and
$\epsilon_2$ = $2\epsilon_o$ (permittivity of shell),

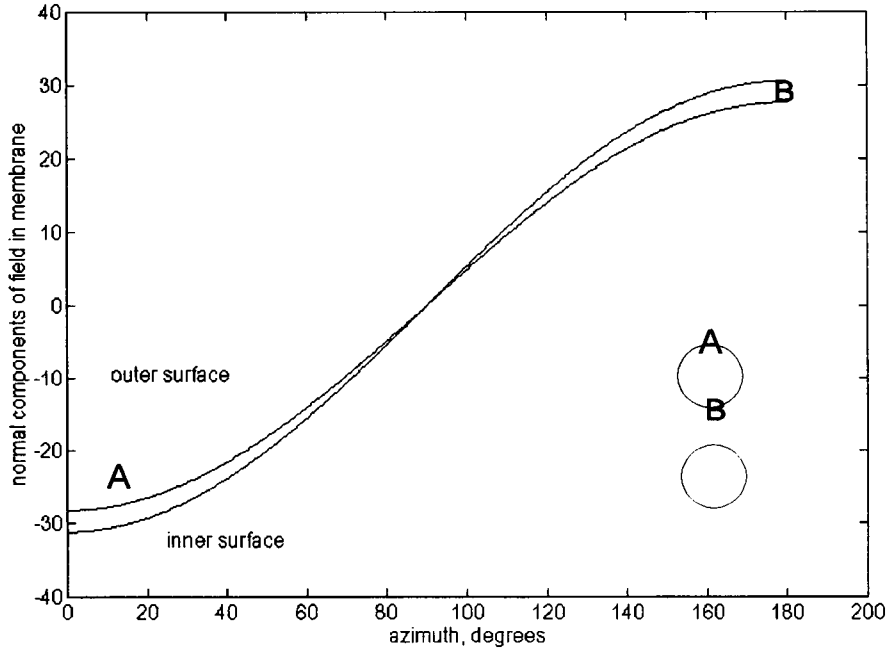


FIGURE 2. Normal components (outer and inner surfaces) of calculated electric fields in the membrane of one of the pair of cells. Normalized cell separation $\gamma = h/r$. Two locations are shown in the inset.

where $\epsilon_0$ ($8.85 \times 10^{-12}$ F/m) is the permittivity of free space. (The results are readily scaled to apply to spheres of typical cellular dimensions.) The net force on the particle was obtained by integrating the force densities over the entire surface of the cell, using Simpson's rule and the program Matlab (The Mathworks, Inc., Natick, MA).

## Membrane fields and potentials

Fig. 2–4 show the calculated electric fields and membrane potentials in the top particle in Fig. 1 versus the azimuthal angle $\theta$. The figures summarize data for one pairs of cells with three different values of the normalized separation $\gamma = h/R$. The separations are: wide ($\gamma = 4$); touching but not fused ($\gamma = 2$); and fused, i.e., touching ($\gamma = 2$) with a channel connecting the inner compartments of the two particles. The diameter of the channel (i.e., the inside diameter of the fusion pore) was 0.5% of the diameter of the cells.

The field distribution and membrane potential in the pair at $\gamma = 4$ are close to those in an isolated cell and in excellent agreement with the analytical solution for Laplace's equation given above. As the cells approach, the field distribution in the membranes shifts progressively. This reduces the field strength in the membrane near the region of closest approach. However, the effect is rather modest, even when the cells are in actual contact (Figs. 3 and 4). When the cells fuse, the membrane potential vanishes near the point of fusion ($150° < \theta < 180°$) but increases by a factor of 1.7 at the opposite poles of the cells ($0° < \theta < 30°$).

## Pressures

As is apparent from Fig. 2, the field strengths in the membrane at the inner and outer surfaces are quite similar; however there is a small difference between them that is responsible for the net force density on the membrane. Moreover, there is a small difference between the net force densities on the opposite ends of the cell that gives rise to the net force of attraction between the two cells.

The net force density on the cells is shown in Fig. 5 and 6. Both the radial (Fig. 5) and the tangential (Fig. 6) forces are directed in a way that would tend to deform the single unfused cells, or fused pair of spheres, into ellipsoids (insets). The forces developed on a fused pair of cells are nearly three times higher than those developed in each of the unfused cells. This is consistent with results of previous experimental and theoretical studies (e.g., Englehardt and Sackmann, 1988; Poznanski et al., 1992).

## Forces between cells

There is a slight asymmetry in the forces on the unfused cells, which results in a net force of attraction between them. Fig. 7 shows the calculated forces of attraction between the cells at various normalized separations $\gamma = h/r$. The forces are normalized by the factor $24\ \pi\ r_{out}\ \epsilon_2/\gamma^4$ (see below). Also shown for comparison are the forces between homogeneous spheres of the same outer diameter as the cells but with a conductivity of zero, or ten times greater than that of the surrounding medium. The forces of attraction between the cells and nonconducting spheres are the same (which is a consequence of the fact that the fields in the external medium in both cases are identical). The attractive force between the conducting spheres is much higher, a consequence of the larger induced dipole moment of the conducting spheres.

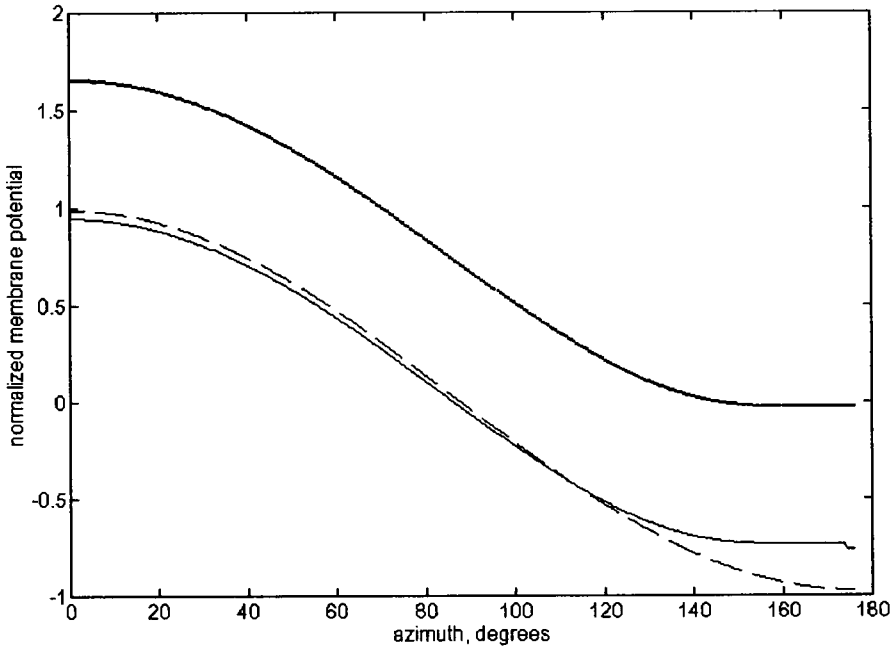


FIGURE 3. Normalized membrane potential. (*Dashed*) Cells separated with $\gamma = 4$; (*thin solid curve*) cells touching; (*thick curve*) cells fused.

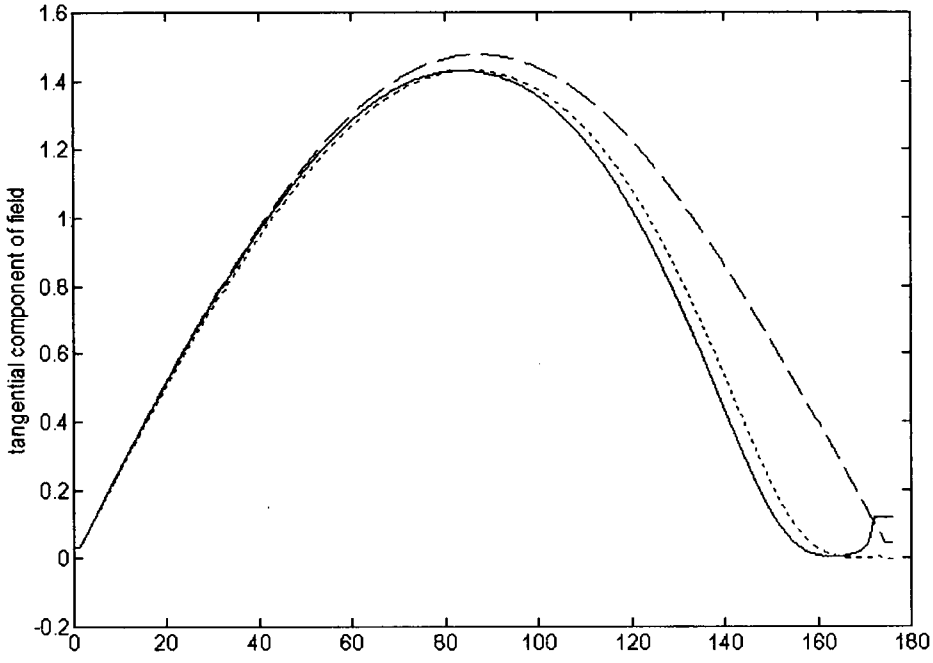


FIGURE 4. Tangential components of electric field at the outer membrane surface. (*Dashed*) $\gamma = 4$; (*dotted*) cells touching; (*solid*) cells fused. The discontinuity near 180 deg for the fused pair is an artifact from the presence of the channel connecting the cells.

### Velocity of approach of two cells

Fig. 8 shows the distance between pairs of red cell ghosts, or of a ghost and either a fused doublet or two unfused cells in contact, versus time. The curves indicate fits to theoretical functions, as described below.

## DISCUSSION

### Changes in fields and forces during electrofusion

As the cells approach each other, the membrane field strength decreases near the point of contact (Figs. 3 and 4). These changes reflect the tendency of the (nonconductive) cells to shield each other near the point of contact as they come into contact. When the cells fuse, there is nearly a threefold increase in the pressure at their poles opposite the fusion zone and a decrease in the net forces at the region of fusion (Fig. 5).

Wu et al. (1994) studied the mechanical responses of a pair of erythrocyte ghosts that had been aligned using an external electric field and fused by a brief high-voltage pulse. Immediately after fusion, the doublet consisted of two nearly spherical halves; it then evolved to nearly spherical shape. Wu et al. reported that the rate of fusion zone expansion depends critically on the field that is used to align the cells, which is clearly a result of dielectrophoretic forces. Inasmuch as the strength of the dielectrophoretic force is very easy to control, further analytical and experimental study may lead to a way to use these mechanical responses to study the mechanics of membranes. Clearly, the forces induced on a fused membrane doublet from dielectrophoresis are substantially higher and in the correct direction to explain the field-accelerated opening of the fusion zone as reported by Wu et al. (1994).

### Forces between the cells

The above results can be used to calculate the forces between the cells. This provides a very sensitive test of the calculations because the forces fall off rapidly with distance and result from cancellation of much larger forces that are exerted by the field on each membrane surface.

For two particles oriented with their line of centers parallel to the field, the interparticle force can be written (Gast and Zukoski, 1989) as

$$f(\gamma) = \frac{24\pi r_{out}^2 u^2 \epsilon_1 \epsilon_0}{\gamma^4} E^2 f_{\|}, \tag{9}$$

where

$$u = \frac{\epsilon_{eff} - \epsilon_1}{\epsilon_{eff} - 2\epsilon_1} \tag{10}$$

is the Clausius–Mossotti function, $E$ is the electric field strength (for alternating fields, the rms field strength) $\epsilon_1$ is the permittivity of the medium, $\gamma$ is the normalized separation of the particles (as used previously), and $\epsilon_{eff}$ is the effective permittivity of the cell. For the present case (lossy media at low frequencies) the permittivities of the cell and medium in Eq. 10 must be replaced by the corresponding conductivities. The correction factor $f_{\|}$ is unity for point dipoles. But, as the particles approach each other, higher-order terms in the interaction become important. The factor $f_{\|}$ has been evaluated numerically by Klingberg (cited in Gast and Zukoski, 1989); an asymptotic expansion for this factor was obtained by Sauer (1985). The numerical results (Fig. 7) agree well with analytical results of Gast and Zukoski and (for low-conductivity particles) with Sauer's approximation.

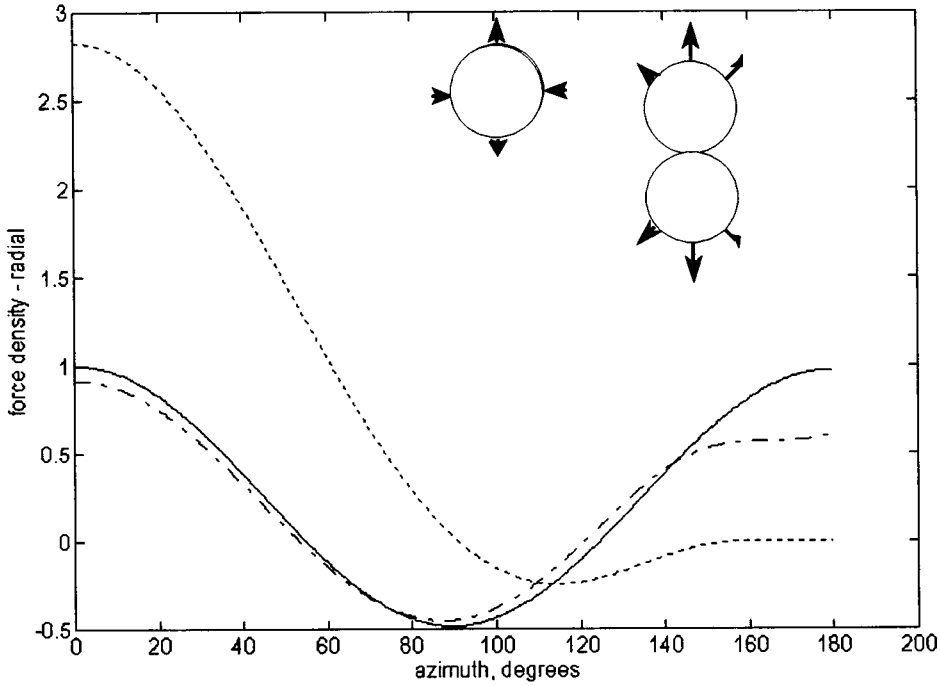


FIGURE 5. Force densities in the radial direction, normalized as described in the text. (*Dotted*) fused cells; (*dotted–dashed*) cells touching; (*solid*) normalized separation $\gamma = 4$. The inset shows the force directions on a single cell and a fused pair.

### *Velocity of approach and intracellular forces*

The third part of this study was intended to clarify the results of Dimitrov et al. (1990), who measured the velocity of attraction between red cell ghosts in an electric field. Using an approximate hydrodynamic model, the investigators deduced a value of $|u| = 0.10$ for the cells, which corresponds to an effective conductivity of the cells that is approximately 75% that of the surrounding electrolyte. Under the conditions of those experiments, the effective conductivity of the cells should be very much smaller than that of the medium, which implies that $u$ should be experimentally indistinguishable from $-0.5$.

To explore this further, we analyze the data in Fig. 8 (which are quite similar to those of Dimitrov et al.) to consider the effect of higher-order terms in the interaction (accounted for $f_1$) or hydrodynamic effects. We base our discussion on Batchelor's theory for the motion of hard spheres under low Reynolds number conditions (Batchelor,

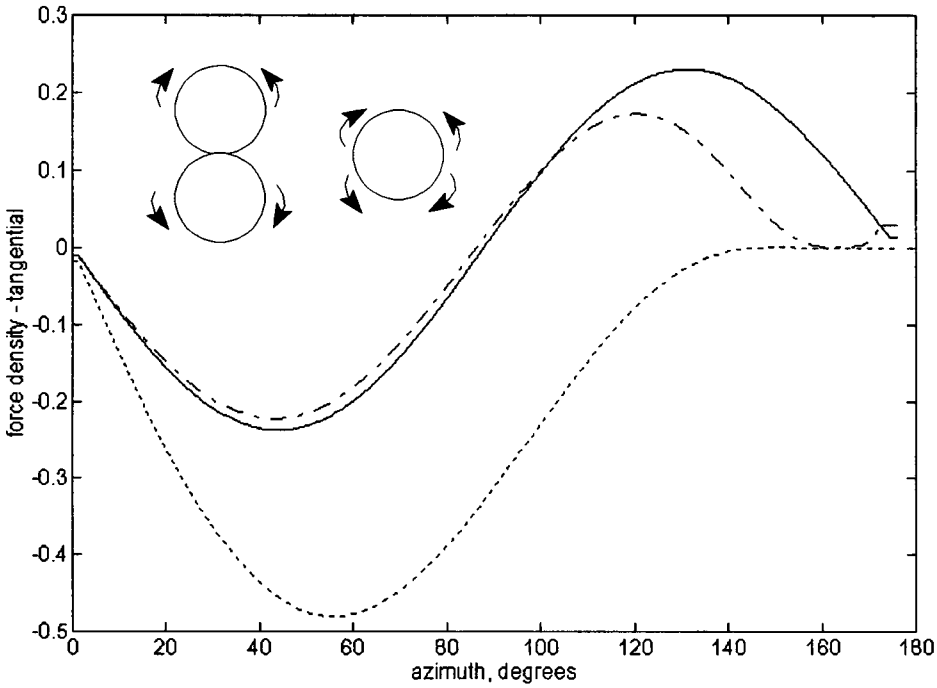


FIGURE 6. Normalized force densities in the tangential direction. (*Dotted*) Fused cells; (*dotted–dashed*) cells touching; (*solid*) cells separated, normalized separation $\gamma = 4$. The insets show the direction of tangential forces in a fused pair and a single cell.

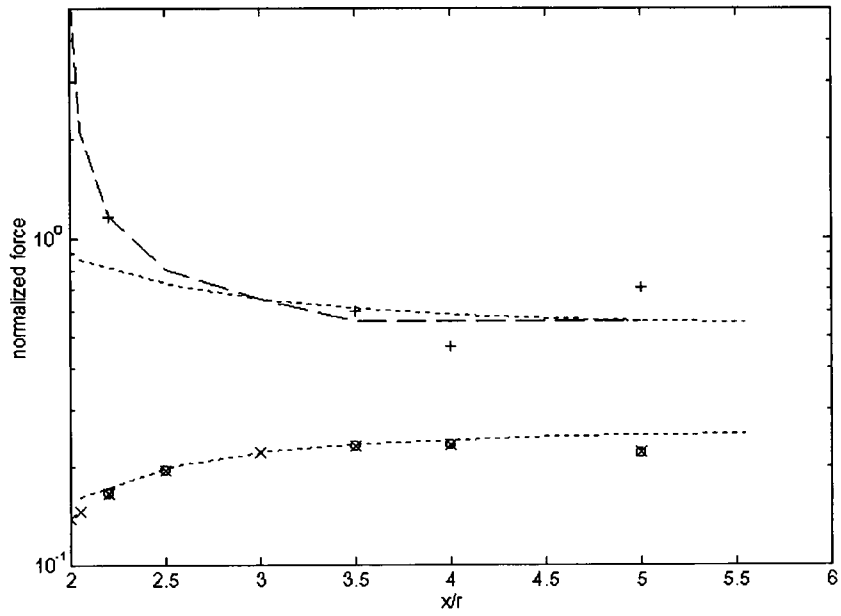


FIGURE 7. Force between (+) conductive spheres ($\sigma_2/\sigma_1 = 10$), (o) nonconductive spheres ($\sigma_2/\sigma_1 = 0$), and (x) shell-surrounded sphere. (–) Multipole expansion; ( . . . ) from Eq. 11.

1976; Russel et al., 1989). In this theory the relative motion of two particles attracted by a force along their line of centers is given by

$$r_{out}\frac{d\gamma}{dt} = -\frac{f(\gamma)}{3\pi\mu r_{out}}(A_{11} - A_{12}), \qquad (11)$$

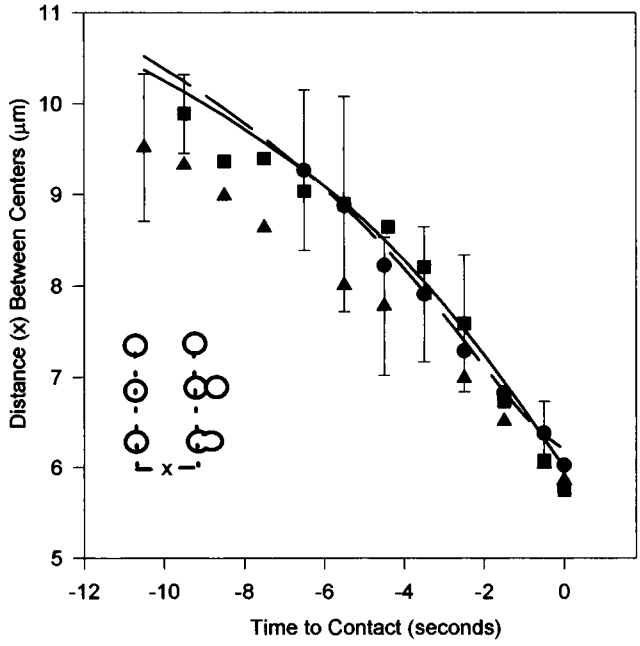


FIGURE 8. Separation versus time of (●) two red cell ghosts ($n = 12$), (▲) a ghost and an unfused doublet ($n = 9$), and (■) a ghost and a fused doublet ($n = 6$). *Solid curve*, hydrodynamic model with asymptotic expansion (Sauer); *dashed curve*, exact hydrodynamic model (Batchelor (1976) fitted to data for two ghosts. Data are averages from $n$ independent measurements for each experimental condition; typical standard deviations are shown. This inset shows the coordinate system used.

where $\mu$ is the viscosity of the medium (0.89 cP for water); the other symbols are the same as defined above. The coefficients $A_{11}$ and $A_{12}$ take into account the hydrodynamic interaction between the particles. As ($\gamma \rightarrow \infty$, $A_{11}$ and $A_{12}$ approach 1 and 0, respectively; in the opposite limit ($\gamma \rightarrow 2$) both coefficients approach 0.775. The first limit corresponds to the classical Stokes law behavior. The second limit implies (by Eq. 11) that the drag on the particles will increase dramatically as the cells come close to contact. Batchelor (1976) tabulated values for $A_{11}$ and $A_{12}$ for two equal spheres from which we obtain data by interpolation in the calculations reported below.

Using the program Mathematica (Wolfram Research, Champaign, IL), we solved Eq. 11 with several different assumptions (Table 1). In each case, we fitted the data for the approach of two red cell ghosts (Fig. 8) to Eq. 11, treating $u$ as the only adjustable parameter. We chose the negative root of $u$, on the assumption that the effective conductivity of the cells is less than that of the medium.

We also consider simplified models, to understand the relative importance of two effects as the cells approach: the departure of the force from inverse-fourth-power behavior (which is due to higher-order terms in the electrical interaction) and hydrodynamic interactions between the cells.

**TABLE 1 Fitted parameters of $u$ for different hydrodynamic models**

| Model | $u$ |
|---|---|
| Neglect hydrodynamic interactions and higher-order terms in electrical force ($A_{11} = 1$; $A_{12} = 0$; $f_{\|} = 1$) | −0.25 |
| Include hydrodynamic interactions (Batchelor, 1976); neglect higher-order terms in force ($f_{\|} = 1$) | −0.42 |
| Include hydrodynamic interactions (Batchelor, 1976) and higher-order terms in force | −0.47 |

The values of $u$ that result from these different assumptions are listed in Table 1. Under the conditions of these experiments, both higher-order electrical and hydrodynamic interactions are important for determining the velocity of approach of the cells. If these effects are taken into account we arrive at a value of $u$ that is very close to the expected value of $-1/2$.

### Velocity of approach of a ghost to a fused or unfused doublet

The results of these experiments are also shown in Fig. 8. The velocity of approach is clearly lower than for individual cells. Unfortunately, in the absence of a hydrodynamic model for these more complicated systems, there is no way to interpret the data rigorously. We note, however, that the dipole moment of an unfused doublet is nearly twice that for a single red cell ghost (Jones and Miller, 1989), and thus the force drawing them together would be twice as high as well. The slower rate of approach is most likely a consequence of a higher hydrodynamic drag.

We reconsider the results of Dimitrov et al. (1990) in light of the present results. Fig. 3 of that paper gives data for the separation versus time of pairs of red cell ghosts in fields of 8 and 16 kV/m, which resemble those in the present study. From those data we find values of $u$ (using Batchelor's model) that are $-0.30$ (8 kV/m) and $-0.24$ (16 kV/m). These values are considerably higher than those obtained from the same data by Dimitrov et al., in part as a consequence of the different hydrodynamic model that was used (Dimitrov, 1983) . Nevertheless, the value of $u$ that we obtain (even with the improved hydrodynamic model) is significantly different from $-1/2$. We suspect that another effect, perhaps deformation of the cells by the (quite strong) electric fields, may have contributed to this result. Experiments of this sort will be sensitive to the electrical properties of the cells only if their effective conductivity is close to that of the medium (cf. Eq. 10). That would require the use of low-conductivity media or the use of high frequencies in cases in which the membranes are short-circuited.

We thank Integrated Engineering Software, Inc., for the use of the program, N. Engheta for helpful discussions about electromagnetic theory, and H. P. Schwan for numerous discussions about the biophysical aspects of the problem. We thank J. D. Rosenberg for technical assistance. This work was supported in part by U.S. Office of Naval Research grant N00014–92-J-1053 and National Institutes of Health grant 1RO3RR07764–01.

## REFERENCES

Batchelor, G. K. 1976. Brownian diffusion of a particles with hydrodynamic interaction. *J. Fluid Mech.* 52:245–268.

Cole, K. S. 1972. Membranes, Ions, and Impulses. University of California Press, Berkeley, CA.

Dimitrov, D. S. 1983. Dynamic interactions between approaching surfaces of biological interest. *Prog. Surf. Sci.* 14:295–424.

Dimitrov, D. S., M. A. Apostolova, and A. E. Sowers. 1990. Attraction, deformation, and contact of membranes induced by low-frequency electric fields. *Biochem. Biophys. Acta.* 1023:389–387.

Englehardt, H., and E. Sackmann. 1988. On the measurement of shear elastic moduli and viscosities of erythrocyte plasma membranes by transient deformation in high frequency electric fields. *Biophys. J.* 54: 495–508.

Foster, K. R. 1993. Electro. (Software review.) *IEEE Spectrum.* 30:16.

Foster, K. R., F. A. Sauer, and H. P. Schwan. 1992. Electrorotation and levitation of cells and colloidal particles. *Biophysical J.* 63:180–190.

Foster, K. R., and H. P. Schwan. 1989. Dielectric properties of tissues—a review. *CRC Crit. Rev. Bioeng.* 17:25–104.

Gast, A. P. and C. F. Zukoski. 1989. Electrorheological fluids as colloidal suspensions. *Adv. Coll. Interface Sci.* 30:153–202.

Grosse, C. and H. P. Schwan. 1992. Cellular membrane potentials induced by alternating fields. *Biophys. J.* 63:1632–.

Jones, T. B., and R. D. Miller. 1989. Multipolar interactions of dielectric spheres. *J. Electrostat.* 22:231–244.

Panofsky, W. K. H., and Phillips, M. 1962. Classical Electricity and Magnetism. Addison-Wesley, Reading, MA. 105–106.

Pastushenko, V. Ph., P. I. Kuzmin, and Yu. A. Chizmadzhev. 1988. Dielectrophoresis and electrorotation of cells: unified theory for spherically symmetric cells with arbitrary structure of membrane. *Biol. Membr. (USSR)* 5:65–77 (in Russian).

Poznanski, J., P. Pawloski, and M. Fikus. 1992. Bioelectrorheological model of the cell 3. Viscoelastic shear deformation of the membrane. *Biophys. J.* 61:612–620.

Russel, W. B., D. A. Saville, and W. R. Schowalter. 1989. Colloidal Suspensions. Cambridge University Press, Cambridge, UK. 44–53.

Saito, M., H. P. Schwan, and G. Schwarz. 1966. Response of nonspherical biological particles to alternating electrical fields. *Biophys. J.* 6: 313–327.

Sauer, F. A. 1983. Forces on suspended particles in the electromagnetic field. *In* Coherent Excitations in Biological Systems. H. Froehlich and F. Kremer, editors. Springer-Verlag, Berlin. 134–144.

Sauer, F. A. 1985. Interaction-forces between microscopic particles in an external electromagnetic field. *In* Interactions between Electromagnetic Fields and Cells. A. Chiabrera, C. Nicolini, and H. P. Schwan, editors. Plenum Press, New York.

Schwan, H. P. 1982. Nonthermal cellular effects of electromagnetic fields: AC-field induced ponderomotoric forces. *Brit. J. Cancer.* 45:Suppl. V, 220–224.

Sowers, A. E. 1993. Membrane electrofusion: a paradigm for study of membrane fusion mechanisms. *Meth. Enzymol.* 220:196–211.

Stratton, J. A., 1941. Electromagnetic Theory. McGraw-Hill, New York.

Winterhalter, M., and W. Helfrich. 1988. Deformation of spherical vesicles by electric fields. *J. Coll. Interface Sci.* 122:583–586.

Wu, Y. K., R. A. Sjodin, and A. E. Sowers. 1994. Distinct mechanical relaxation components in pairs of erythrocyte-ghosts undergoing fusion. *Biophys. J.* 66:114–119.